PARENTAL MELT OF NAKHLITES AS DETERMINED FROM MELT INCLUSIONS. A. M. Ostwald[1], A. Udry[1], and J. Gross[2], [1]University of Nevada, Las Vegas, 4505 S Maryland Pkwy, Las Vegas NV 89154; ostwald@unlv.nevada.edu, [2]Rutgers University, 610 Taylor Road, Piscataway, NJ 08854; jgross@eps.rutgers.edu.

Introduction: The nakhlite and chassignite martian meteorites, which are ~1.3 Ga old, augite-rich cumulates and dunites, respectively, consist of 16 samples, and are the largest sample suite from a single location on Mars [1]. Nakhlites and chassignites, therefore, provide unparalleled insight into recent martian volcanism. Determining the parental melt composition(s) of chassignites and nakhlites could reveal the degree of heterogeneity of the martian mantle. As the bulk composition of cumulate rocks cannot represent their parental melts, methods including mass balance calculations, as well as determination of melt inclusion composition by either experimental rehomogenization or *in situ* elemental analyses, are used to estimate parental melt compositions instead [2]. Prior studies have shown that both olivine- and pyroxene-hosted melt inclusions in Nakhla, as well as pyroxene-hosted melt inclusions in Miller Range (MIL) 03346 are enriched in K_2O, likely due to metasomatism of the nakhlite and chassignite source rock prior to partial melting and ascent [2,3].

Of the very few studies that attempt to estimate the nakhlite parental melt (NPM) only three are nakhlites: Nakhla [e.g., 2,4-7], Governador Valadares [4], and MIL 03346 [3]. Other studies [e.g., 1, 8] find isotopic and textural heterogeneity among the nakhlites, possibly indicating that nakhlites originate from multiple parental melts. Constraining the parental magma composition and the effect of metasomatism on both olivine- and pyroxene-trapped liquids in additional samples is crucial to understanding the petrogenetic history of nakhlite and chassignite meteorites. Here, we present new parental melt compositions of the nakhlites MIL 090030 and MIL 090032 based on 5 olivine-hosted melt inclusions. Parental melt composition calculations of Northwest Africa (NWA) 10645, NWA 11013, Caleta el Cobre (CeC) 022, Chassigny, NWA 2737, and Governador Valadares are currently ongoing. Of these, NWA 10645, NWA 11013, and CeC 022 are recent finds, and have never been analyzed for their parental melts. In addition, Righter et al. [8] suggest that NWA 10153, possibly paired with NWA 11013, originate from a different source than the other nakhlites; characterizing the NWA 11013 parental melt, thus, may aid in identifying their source(s).

Methods: Olivine-hosted melt inclusions in MIL 090030,21 and MIL 090032,21 are complex and include micro-crystalline phases. All melt inclusions were analyzed with a 15 kV accelerating voltage and 10 nA beam current (to avoid migration of volatile elements). The micro-crystalline phases were too small for single analyses; a defocused (5 μm) beam was used to obtain bulk analyses of the melt inclusions instead. Only a single melt inclusion (MIL 090032 Ol-MI01, Fig. 2b) had large enough phases to allow for individual spot analysis with a focused beam (1 μm): one was a high-Si phase, and the other consisted of micro-crystalline pyroxene dendrites in a glassy matrix. All host minerals (pyroxene and olivine) were analyzed with a 15 kV accelerating voltage, 20 nA current, and 2 μm beam diameter.

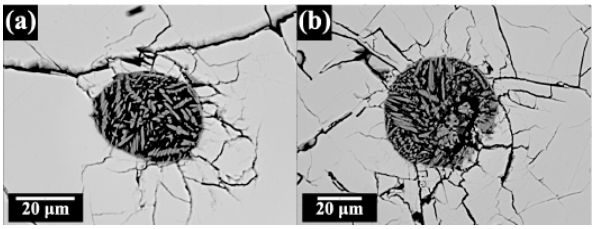

Figure 1: Olivine-hosted melt inclusions in MIL 090030. Inclusion (a) is MIL 090030 Ol-MI01, and (b) is MIL 090030 Ol-MI02.

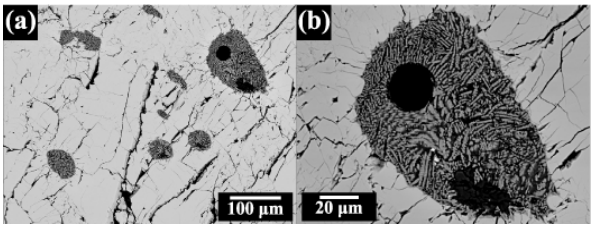

Figure 2: (a) Olivine-hosted melt inclusions in MIL 090032. *(b)* MIL 090032 MI01.

Olivine-Hosted Melt Inclusion Petrography: Olivine-hosted melt inclusions in Miller Range are typically small (~50 μm), with only one inclusion (MIL 090032_Ol-MIO1) as large as 100 μm. All of the observed olivine-hosted melt inclusions are complex, with concentric micro-crystalline (<1-2 μm) crystals of pyroxene radiating inward from the inclusion walls, all contained in a glassy matrix (Figs. 1 and 2). Some melt inclusions (MIL 090032 Ol-MIO1 and Ol-MIO2) contain late-stage phases (Fe-Ti oxides), indicating early entrapment of melt. Furthermore, as late-stage phases occur in the central portions of melt inclusions, their presence ensures a representative, rather than an off-center, cut. Olivine has a core-to-rim composition of Fo_{43-31}, with an average composition of Fo_{42} in olivine cores.

Olivine-Hosted Parental Melt Reconstruction: As olivine-hosted melt inclusions cool, olivine crystallizes on the inclusion wall and reequilibrates

with the host, typically resulting in a net "Fe-loss" in the trapped melt [9]. The modeling software PETROLOG3 reverses this process, requiring a known value for the initial FeO_T of the parental melt and the Fo value of the host olivine [9]. We selected our FeO_T values from three proposed NPM calculations from previous studies: FeO_T=26.9 wt.% was determined by experimental rehomogenization of augite with melt inclusions, concluding that olivine and pyroxene co-evolved and finding low K_2O contents (~0.39 wt.%) [7]. Two other studies used *in situ* elemental microanalyses of augite-hosted inclusions in MIL 03346 (FeO_T=22.2 wt.%) [3], and of olivine-hosted inclusions in Nakhla (FeO_T=28.9 wt.%) [2]. Both studies using *in situ* analyses found high K_2O contents (~1.8 wt.%) after correcting for re-equilibration.

In this study, the cores of host olivines in both MIL 090030 and MIL 090030 have $Fo_{\sim 42}$, which agrees with previous studies [3,10]. Miller Range nakhlites cooled quickly [10,11] and thus it can be assumed that there was little reequilibration of the olivine cores. Therefore, a starting olivine core composition of Fo_{42} can be safely assumed.

Results and Discussion: Modal abundances of the two MIL 090032 Ol-MI01 phases were determined using *ImageJ* software, and totaled 93.5% glass/pyroxene and 6.5% of the high-Si phase. The calculated present bulk composition (PBC) for each of our melt inclusions ranges 51.8–61.6 wt.% SiO_2, 10.5–14.6 wt.% Al_2O_3, 6.1–16.0 wt.% FeO, 0.5–2.6 wt.% MgO, 7.6–14.7 wt.% CaO, 0.7–1.7 wt.% K_2O, 1.9–4.3 wt.% Na_2O and 0.1–0.2 wt.% Cl. Only Cr_2O_3 was consistently below detection limits. We found a range of K_2O contents between 0.5 and 1 wt.% in our corrected melts, which are not as high as the K_2O values reported for olivine-hosted inclusions in Nakhla, or augite-hosted inclusions in MIL 03346 (~1.8 wt.%) (Fig. 3). Furthermore, Na_2O concentrations in the PTL ranging from 1.3–3.0 wt.%, compared to a value of ~1 wt.% in olivine-hosted inclusions in Nakhla and pyroxene-hosted inclusions in MIL 03346 (Fig. 4).

The discrepancies in NPM between this study and previous studies [2,3] could: (1) represent sampling error or (2) be indicative of heterogeneity among PTLs in nakhlites and could suggest multiple parental melts among the suite. Furthermore, we find that different parental melts are enclosed by pyroxene and olivine in nakhlites, signifying dissimilar magmatic processes occurring during crystallization of each phase. Although nakhlites and chassignites are related [e.g. 1], the relationship between their parental melts remains unclear. A larger study encompassing both olivine- and augite-hosted melt inclusions in the nakhlites, as well as olivine-hosted melt inclusions in chassignites, is warranted.

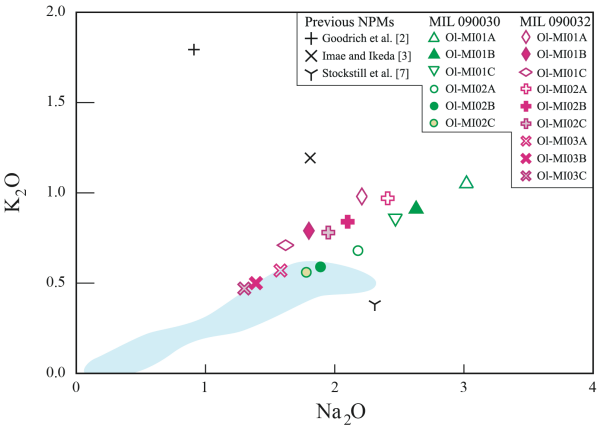

Figure 3: Na_2O plotted against K_2O for each reconstructed parental melt. A denotes an FeO_T of 22.2% [3], B denotes an FeO_T of 26.9% [7], and C denotes an FeO_T of 28.9% [2]. Blue envelope indicates bulk nakhlite compositions [1].

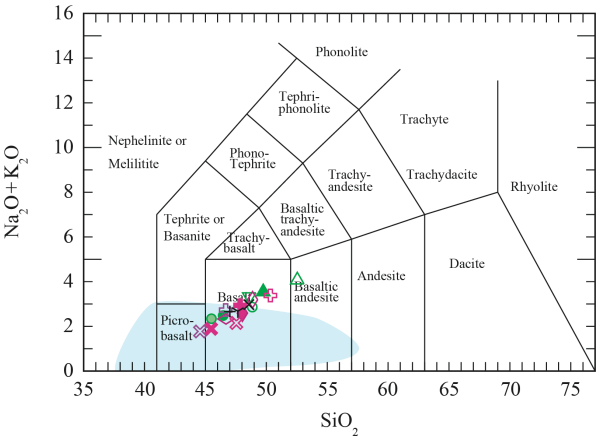

*Figure 4:*A total alkali versus silica (TAS) diagram of each of the reconstructed trapped liquids for both MIL 090030 and MIL 090032. Blue envelope indicates bulk nakhlite compositions [1].

References: [1] Udry, A., and Day, J.M.D. (2018) *GCA, 238,* 292-315. [2] Goodrich, C.A. et al. (2013) *Meteoritics & Planet. Sci., 48,* 2371-2405. [3] Imae, N. and Ikeda, Y. (2007) *Meteoritics & Planet. Sci., 42,* 171-184. [4] Harvey, R.P., and McSween, H.Y. (1992) *Earth & Planet. Sci., 111,* 467-482. [5] Treiman, A.H. (1993) *GCA, 57,* 4753-4767. [6] Sautter, V. et al. (2012) *Meteoritics & Planet. Sci., 47,* 330-344. [7] Stockstill, K.R. et al. (2005) *Meteoritics & Planet. Sci., 40,* 377-396. [8] Righter, M., et al. (2016) *LPSC XLVII*, Abstract #2780. [9] Danyushevsky, L.V. and Plechov, P. (2011) *Geochem GeophysGeosys, 12, No. 7.* [10] Day, J.M.D, et al. (2006) *Meteoritics & Planet. Sci., 41,* 581-606. [11] Udry, A. et al. (2012) *Meteoritics & Planet. Sci., 47,* 1575-1589.